

The Effect of the Calculation of Slip Speed on the Wear of Wheel Profiles: A Benchmarking Against the SIMPACK Wheel Profile Wear Module

*Original*

The Effect of the Calculation of Slip Speed on the Wear of Wheel Profiles: A Benchmarking Against the SIMPACK Wheel Profile Wear Module / Magelli, M., Zampieri, N., Bosso, N.. - In: CIVIL-COMP CONFERENCES. - ISSN 2753-3239. - 7:(2024), pp. 1-11. (Sixth International Conference on Railway Technology: Research, Development and Maintenance (RAILWAYS 2024) Prague (CZ) 1-5 September 2024) [10.4203/ccc.7.9.2].

*Availability:*

This version is available at: 11583/3008072 since: 2026-03-02T10:48:35Z

*Publisher:*

Civil-Comp Press

*Published*

DOI:10.4203/ccc.7.9.2

*Terms of use:*

This article is made available under terms and conditions as specified in the corresponding bibliographic description in the repository

*Publisher copyright*

(Article begins on next page)



Proceedings of the Sixth International Conference on  
Railway Technology: Research, Development and Maintenance  
Edited by: J. Pombo  
Civil-Comp Conferences, Volume 7, Paper 9.2  
Civil-Comp Press, Edinburgh, United Kingdom, 2024  
ISSN: 2753-3239, doi: 10.4203/ccc.7.9.2  
©Civil-Comp Ltd, Edinburgh, UK, 2024

# **The Effect of the Calculation of Slip Speed on the Wear of Wheel Profiles: A Benchmarking Against the SIMPACK Wheel Profile Wear Module**

**M. Magelli, N. Zampieri and N. Bosso**

**Department of Mechanical and Aerospace Engineering,  
Politecnico di Torino  
Italy**

## **Abstract**

The efficiency of modern computers in the solution of railway vehicle dynamics with multibody codes is currently leading the path towards the development of numerical tools for the evaluation of wear of the wheel profiles starting from the outputs of dynamic simulations. The latter are commonly launched in commercial software packages, which guarantee unbeaten reliability and stability of their numerical solvers, as well as simple user-friendly interfaces. Many commercial multibody codes are currently provided with add-ons for the evaluation of wear of wheel profiles, however the limited number of tuneable parameters can compromise the stability of the simulation. The present paper aims to benchmark the outputs of the SIMPACK Wheel Profile Wear module and to investigate the differences due to the application of the Archard's law in local form, focusing on different strategies that can be adopted to calculate the slip speed on the contact patch with the FASTSIM algorithm. It is found that recent expressions suggested in the literature for the calculation of the equivalent flexibility should be preferred over the original equation when calculating the slip speed in each cell of the contact patch grid.

**Keywords:** multibody simulation, railway vehicle dynamics, wear, SIMPACK, wheel-rail contact, co-simulation.

## **1 Introduction**

Railway companies have shown a growing interest towards the numerical simulation of wear of the wheel profile shapes, which has thrust the production of several

works on the topic in recent years [1-4]. In fact, the prediction of the evolution of wear of wheel profiles with numerical codes can support (i) the optimized scheduling of returning maintenance operations [5], (ii) the identification of optimized profile shapes, hence extending the operating life of wheels [6,7], and (iii) the assessment of the vehicle dynamic behaviour with worn profiles at the earliest stages of the vehicle design.

The calculation of the worn profile shape mainly requires the simulation of the vehicle-track interaction, including the solution of the wheel-rail contact problem in each time step, and the definition of a suitable wear law to relate the amount of worn material to the main quantities related to the wheel-rail contact. The first task can be effectively solved through multibody (MB) simulations, while the second task can be implemented in the form of a wear model receiving as inputs the main results of the MB simulation. Nowadays, commercial MB software packages include built-in modules for the estimation of the worn material and worn profile shape, thus allowing the users to easily calculate wear from the results of the dynamic simulation. Although commercial MB codes are often the preferred solution to launch dynamic simulations, in view of their high reliability and of the numerical stability of their numerical integrators, their wear modules offer limited customization to the users. This can threaten the stability of the computation, especially in simulations requiring the subsequent replacement of the profiles with worn shapes to simulate the dependency of vehicle dynamics on wear [8]. Therefore, the development of external routines for the calculation of the worn material and the determination of the worn profile shape can be the key to gain control over the computation and improve the stability of the simulation. Such wear routines post-process the outputs of the dynamic simulation and can benefit from co-simulation techniques [9] to improve the computational efficiency of the whole simulation framework.

The present paper aims to validate in-house wear routines against the outputs of the wear module of the SIMPACK commercial MB code (SIMPACK Wheel Profile Wear module), thus gaining further insights into the capabilities of the commercial wear module. More in detail, the paper aims to compare the differences between the global approach in the application of the wear laws, followed by the SIMPACK Wheel Profile Wear module, and a local strategy, investigating the effect of different modelling parameters in the solution of the wheel-rail contact problem with the FASTSIM algorithm.

## **2 Methods**

To benchmark the outputs of the wear routines, the present paper establishes a numerical framework that relies on a dynamic simulation run with the SIMPACK MB code. The outputs of the simulation, mainly the results of the wheel-rail contact problem in each time step, are then processed with different wear routines to calculate the normal wear depth along the profile, which can then be used to determine the worn profile shape. The wear routines include the SIMPACK Wheel Profile Wear module and the external in-house MATLAB routines under validation.

As the paper mainly aims to compare different wear routines, rather than accurately predict the wear on a specific line, the dynamic simulation considers a generic mission of a Aln663 passenger diesel railcar running on a reference track, which does not correspond to a specific line, but it is built to assess the performances of the wear routines in a scenario with high tortuosity, see Figure 1. In fact, the reference track is 20 km long, and it includes 38 curves, i.e., 19 left-handed (RH) curves with radius in the range 200-2000 m, with step of 100 m, followed by the same curves in right-handed (RH) direction, see Figure 1b)-c). The reference vehicle is chosen to be the Aln663 diesel railcar since this passenger vehicle proved to suffer from large wear when running on mountain tracks in Northern Italy. The curve superelevation and speed profile mission are selected to comply with the limits on the maximum vehicle speed (120 km/h) and unbalanced acceleration ( $0.6 \text{ m/s}^2$ ) as prescribed the Italian Railway Administration (RFI). All bodies in the vehicle MB model are treated as rigid, and they include one coach, 2 bolsters, 2 FIAT bogie frames, 8 axle-boxes and 4 wheelsets, see Figure 1a). The axle-box bodies only feature a rotational degree of freedom (DOF) with respect to the wheelset on which they are mounted, while for all other bodies, the SIMPACK “Generail Rail Track Joint” is applied, which prescribes 6 DOFs defined with respect to the track direction. The track is modelled as rigid and without irregularities, to exclude the effect of stochastic parameters on the preliminary benchmarking of the wear functions. The wheel and rail profiles considered in the model are the S1002 wheel profile and the UIC60 rail profile. Further details on the model can be found in [9].

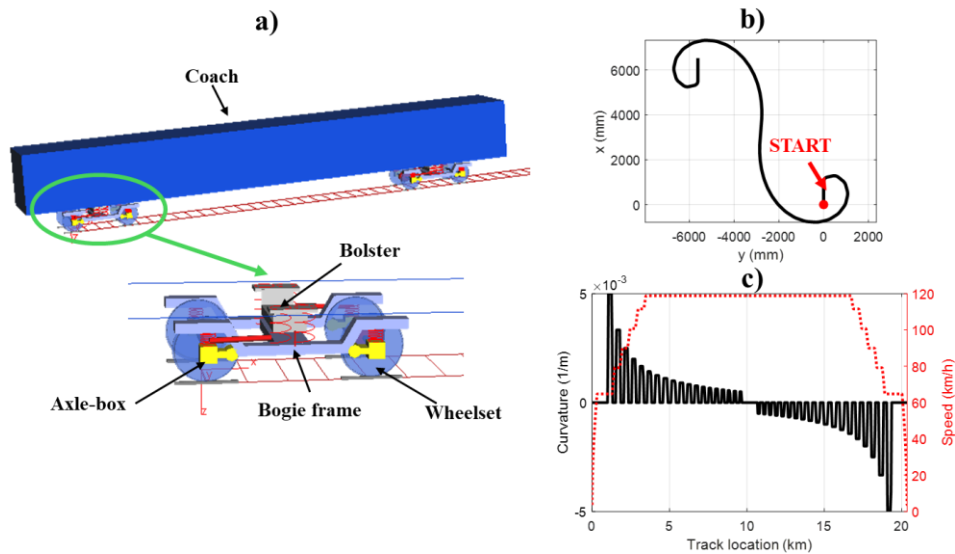


Figure 1: Reference MB model: a) vehicle, b) track layout and c) Track curvature and speed profile along track.

The wheel-rail contact is solved in SIMPACK using the equivalent elastic method, which is based on a virtual penetration method to identify a non-Hertzian contact patch, which is then turned into an equivalent ellipse. The tangential problem is subsequently solved using the default FASTSIM [10] routine available in SIMPACK. Although SIMPACK also includes a discrete elastic method, which keeps the non-

elliptic patch for the calculation of the tangential forces, the equivalent elastic method is selected since it ensures a faster computation and since the goal of the paper is to simply compare the outputs of different routines from the same inputs.

The results of the MB simulations are post-processed with dedicated routines to evaluate the amount of worn material at the end of the mission simulated in SIMPACK. The wear routines include (i) the SIMPACK Wheel Profile Wear add-on, (ii) a MATLAB routine trying to mimic the outputs of the SIMPACK wear module and (iii) a MATLAB routine based on a local application of the wear laws. The SIMPACK Wheel Profile Wear module calculates wear using a global approach, i.e., the total amount of worn volume is evaluated from the global forces and creepages at the contact patch, thus not requiring the discretization of the contact patch into adhesion and slip areas for the sake of wear evaluation. SIMPACK offers two laws, namely the Archard's wear law and the Krause-Poll law. In the present paper, only the Archard's law is considered because it is more solid in the literature. According to Archard's law, the wear volume on the wheel  $\Delta V_w$  is evaluated as stated by Equation (1):

$$\Delta V_w = \frac{k_{Arch}(v_s, p_z)}{2} \cdot \frac{N d_s}{H} \quad (1)$$

where N is the normal load,  $d_s$  is the sliding distance, H is the hardness of the softer material and  $k_{Arch}$  is the wear coefficient, which is typically evaluated from experimental maps as a function of sliding speed  $v_s$  and average normal contact pressure  $p_z$ . In this paper, the experimental map suggested by Swedish researchers from Royal Institute of Technology (KTH) is adopted [11], which considers four wear regions. An average value of wear coefficient for each wear zone is defined in this work, as SIMPACK only allows to specify a single wear coefficient in each zone, and it cannot deal with a full map. Table 1 defines the wear coefficients and the boundaries of each zone considered for this work. It is interesting to highlight that the wear coefficients defined in SIMPACK should be doubled with respect to the values suggested by KTH researchers, as SIMPACK automatically calculates the total worn volume and then spreads 50% to the wheel and 50% to the rail.

Wear zone	Wear coefficient	Zone boundaries
Mild 1	1.43e-4	$p_z < 0.8H$ & $v_s < 0.2$ m/s
Severe	1.00e-3	$p_z < 0.8H$ & $0.2 < v_s < 0.7$ m/s
Mild 2	1.43e-4	$p_z < 0.8H$ & $v_s > 0.7$ m/s
Seizure	1.00e-2	$p_z > 0.8H$

Table 1: MBS model eigenvalues.

Equation (1) only calculates the total amount of wear volume on the contact patch, but the corresponding distribution of normal wear depth should be calculated to obtain the worn profile. As no information is provided by SIMPACK documentation about the algorithm used to spread the total worn volume, a MATLAB routine was developed in past works [12] to reproduce the calculation made by SIMPACK. The

MATLAB global routine assumes the distribution of normal wear depth to be proportional to the Hertzian contact pressure on the equivalent ellipse, so it is a semi-elliptic distribution as stated by Equation (2):

$$\Delta z_n(y) = \frac{2}{\pi b} \cdot \frac{\Delta V_w}{2\pi R_{cp} \cos \delta} \sqrt{1 - (y/b)^2} \quad (2)$$

where  $y$  is the lateral coordinate on the contact patch,  $b$  is the lateral semi-axis of the equivalent contact ellipse,  $R_{cp}$  is the contact radius and  $\delta$  is the contact angle calculated from the profile tangent.

The main drawback of the calculation of wear with a global approach is that the resultant wear depth distribution must be assumed a priori, thus not accounting for the real distinction between adhesion and slip areas. Moreover, when wear is spread proportionally to the contact pressure, the maximum wear peak coincides with the point featuring the maximum pressure, whereby the adhesion limit may not be overcome. Therefore, a more accurate calculation of wear can be obtained if the wear depth is calculated in each element of the contact patch grid with the application of Archard's law in local form, see Equation (3):

$$\Delta z_n(x, y) = \frac{k_{Arch}(w(x, y), p_z(x, y))}{2} \cdot \frac{p_z(x, y)u(x, y)}{H} \quad (3)$$

where the contact pressure  $p_z$ , slip speed  $w$  and sliding distance  $u$  are calculated in each element of the contact patch grid located at the coordinates  $(x, y)$  in rolling and lateral directions, respectively. To finally obtain the normal wear depth distribution along the lateral coordinate, the wear depth distribution calculated with Equation (3) must be summed along each longitudinal strip and then spread along the circumferential direction, see Equation (4):

$$\Delta z_n(y) = \frac{1}{2\pi R_{cp}} \int_{-a}^a \sqrt{1 - (y/b)^2} \Delta z_n(x, y) dx \quad (4)$$

where  $a$  is the longitudinal semi-axis of the contact ellipse. It is evident that the greater accuracy of the local method involves a reduction of the computational times of the wear module, since the local distribution of slip speed is needed to compute the wear depth. In this paper, the MATLAB local wear model includes a routine implementing the original FASTSIM algorithm to evaluate the distribution of tangential pressure and slip speed over the contact patch. The in-house FASTSIM algorithm is validated against the outputs predicted by the function available in SIMPACK.

It is well known that the FASTSIM algorithm can efficiently solve the tangential contact problem under the hypothesis that the elastic displacement is proportional to the tangential contact pressure through a flexibility parameter. In the original FASTSIM paper [10], Kalker suggested to transform the contact area into the circle with unitary radius, thus accordingly converting the values of creepages, sliding distance and sliding speed into non-dimensional quantities based on the values of three different flexibility parameters, calculated from the linear theory. Therefore, the equivalent creepages on the unitary radius circles should be calculated as:

$$n_x = \frac{a\xi}{\mu p_{z,0} L_1}; n_y = \frac{a\eta}{\mu p_{z,0} L_2}; f_x = \frac{ab\varphi}{\mu p_{z,0} L_3}; f_y = \frac{a^2\varphi}{\mu p_{z,0} L_3} \quad (5)$$

where  $n_x$ ,  $n_y$ ,  $f_x$  and  $f_y$  are the equivalent creepages,  $\xi$ ,  $\eta$ ,  $\varphi$  are the original creepages in longitudinal, lateral and spin direction,  $\mu$  is the friction coefficient,  $p_{z,0}$  is the maximum normal contact pressure and finally coefficients  $L_i$  with  $i = 1-3$  are the flexibility parameters. Consequently, the scaled sliding speed vector could be calculated as:

$$\mathbf{w}' = \begin{Bmatrix} w'_x \\ w'_y \end{Bmatrix} = \begin{Bmatrix} n_x - y' f_x - \frac{\partial p'_x}{\partial x'} \\ n_x + x' f_y - \frac{\partial p'_y}{\partial x'} \end{Bmatrix} \quad (6)$$

where quantities with apex refer to scaled quantities, and  $p_x$  and  $p_y$  refer to the tangential contact pressure in longitudinal and lateral directions. Kalker then defined a scaling factor for the magnitude of the slip speed, based on an equivalent flexibility parameter, as stated by Equation (7):

$$w' = \|\mathbf{w}'\| = \frac{aw}{\mu p_{z,0} L_{eq} v_{ref}} \quad (7)$$

where  $v_{ref}$  is the reference rolling speed and  $L_{eq}$  is the equivalent flexibility. For the latter, the original expression provided by Kalker is stated by equation (8).

$$L_{org} = \frac{|\xi|L_1 + |\eta|L_2 + \sqrt{ab}|\varphi|L_3}{\sqrt{\xi^2 + \eta^2 + ab\varphi^2}} \quad (8)$$

Nonetheless, Vollebregt and Voltr [13] recently pointed out that the original expression of the equivalent flexibility is not suitable for mixed creepage conditions, and they proposed additional expressions, i.e., the linear weight expression in equation (9) and the squared weight expression in equation (10).

$$L_{lin} = \frac{|\xi|L_1 + |\eta|L_2 + \sqrt{ab}|\varphi|L_3}{|\xi| + |\eta| + \sqrt{ab}|\varphi|} \quad (9)$$

$$L_{sqr} = \frac{\xi^2 L_1 + \eta^2 L_2 + ab\varphi^2 L_3}{\xi^2 + \eta^2 + ab\varphi^2} \quad (10)$$

The MATLAB routines based on the local application of the Archard's law are tuned considering either three separate flexibilities to calculate the magnitude of the sliding speed or a single equivalent flexibility. With three flexibilities, the dimensional components  $w_x$  and  $w_y$  are calculated using independent scaling factors for  $n_x$ ,  $n_y$ ,  $x'$ ,  $y'$ ,  $f_x$  and  $f_y$ , see Equation (5). On the other hand, when a single equivalent flexibility parameter is adopted, the magnitude of the dimensional sliding speed is calculated with Equation (7), starting from the magnitude of the non-dimensional sliding speed  $w'$ . For this latter case, the expressions for the calculation of the equivalent flexibility provided by Kalker, see Equation (8), as well as those suggested by Vollebregt and Voltr, are all tested and compared with the outputs provided by SIMPACK. Regardless of the expressions used to evaluate the slip speed magnitude, the sliding distance is calculated according to Equation (11):

$$u(x, y) = \frac{w(x, y)}{v_{ref}} \cdot \Delta x \quad (7)$$

where  $\Delta x$  is the size of the contact patch element in rolling direction.

### 3 Results

The developed wear routines are compared in terms of the distribution of the normal wear depth along the lateral coordinate of the wheel profile at the end of the reference mission simulated with the SIMPACK commercial MB code. Wear is calculated on both wheels of the leading wheelset, however, due to the symmetric track and vehicle models, the results for left and right wheels are overlapping each other. Therefore, results are presented here for the left wheel only, but the same considerations can be easily extended to the right wheel.

Figure 2 shows the results obtained with the different wear routines tested in this work, i.e., the SIMPACK Wheel Profile Wear module, the MATLAB routine aiming to replicate the results obtained by SIMPACK and the MATLAB local routine that uses three separate flexibilities for the calculation of the slip speed. Figure 2 shows that the largest wear is obtained on the flange, as the contact conditions on the flange when negotiating a curve are more severe. It can be confirmed that the MATLAB global routine calculates output that overlap the results provided by the SIMPACK Wheel Profile Wear module, and this proves that spreading the wear volume according to the Hertzian contact pressure is the path followed by the SIMPACK algorithm.

A comparison between the local and global approach suggests that the two methods provide similar results, but the local approach calculates slightly higher peaks on the flange. In contrast, the results of the local method seem slightly shifted with respect to the outputs provided by SIMPACK on the tread. The explanation to this behaviour is that the local method can predict a separate wear zone in each element of the grid, while the global method can only assign a single wear regime to the whole patch. Therefore, when the contact is on the flange and the slip area is extended to the whole patch, some elements can fall into the severe regime, thus leading to an overall higher wear in this part of the profile. Conversely, when the contact point is on the tread, a large portion of the contact patch is in adhesion condition, hence not contributing to wear. Consequently, the wear depth predicted by the local method is lower and the location of material removal is different when compared to the global algorithm. Furthermore, the global approach can produce local peaks that may threaten the stability of the simulation when cascades of wear simulations are launched. These peaks are obtained when the number of contact points abruptly changes during the simulation, so that the contact patch area is small, and the pressure jumps to values corresponding to the seizure regime. The local approach does not foresee such peaks, as when the contact pressure is high, the adhesion limit is not overcome, and no material removal is predicted. A detailed

data analysis showed that the numerical peaks provided by the global method can be removed with slight changes to the wear algorithm and with a modification of the damping term in the calculation of the normal force performed by SIMPACK during the dynamic simulation.

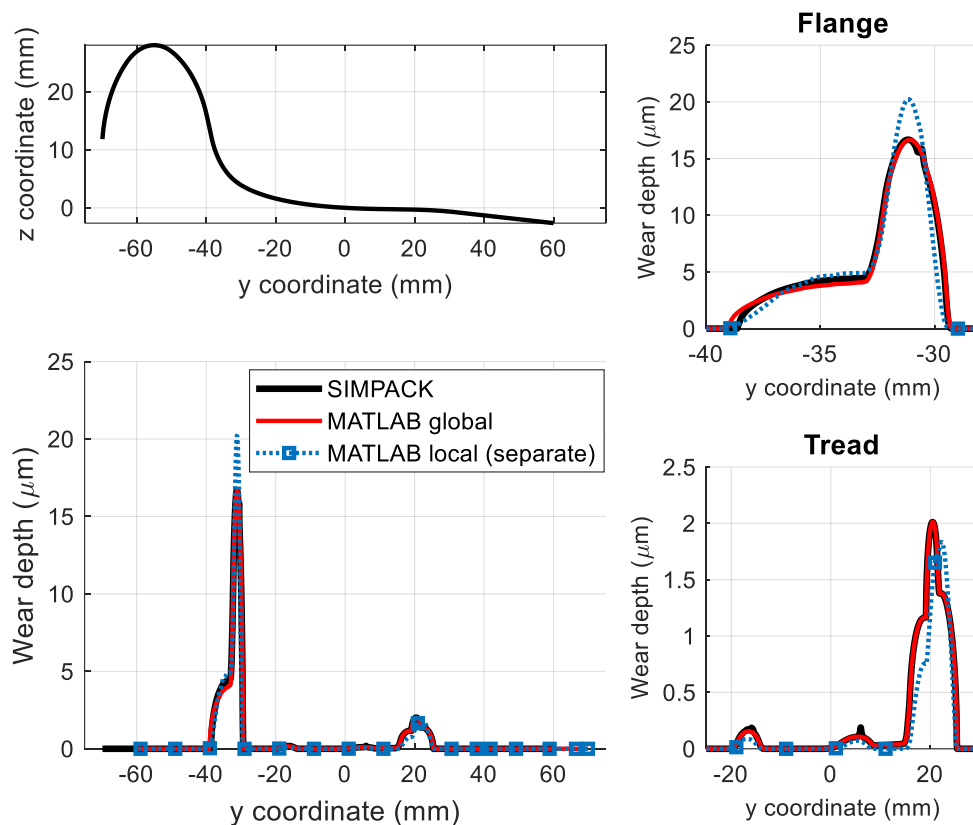


Figure 2: Comparison of local and global routines with zooms on flange and tread.

Concerning the results of the local routine, additional simulations are run to investigate the effect of the different strategies used to compute the magnitude of the slip speed. The results are given in Figure 3, which shows that the wear depth calculated with the original expression by Kalker for the equivalent flexibility deviates from the outputs of all other routines. This is because when using Equation (8) for the evaluation of the equivalent flexibility, the sliding speed magnitude calculated with Equation (7) increases at large spin values, thus predicting severe wear, whereby the Archard's coefficient is about 7 times higher with respect to the mild regime according to Table 1. Conversely, the results obtained with the expressions suggested by Vollebregt and Voltr agree well with each other and with the wear depth distribution obtained using three separate flexibilities to evaluate the slip speed magnitude.

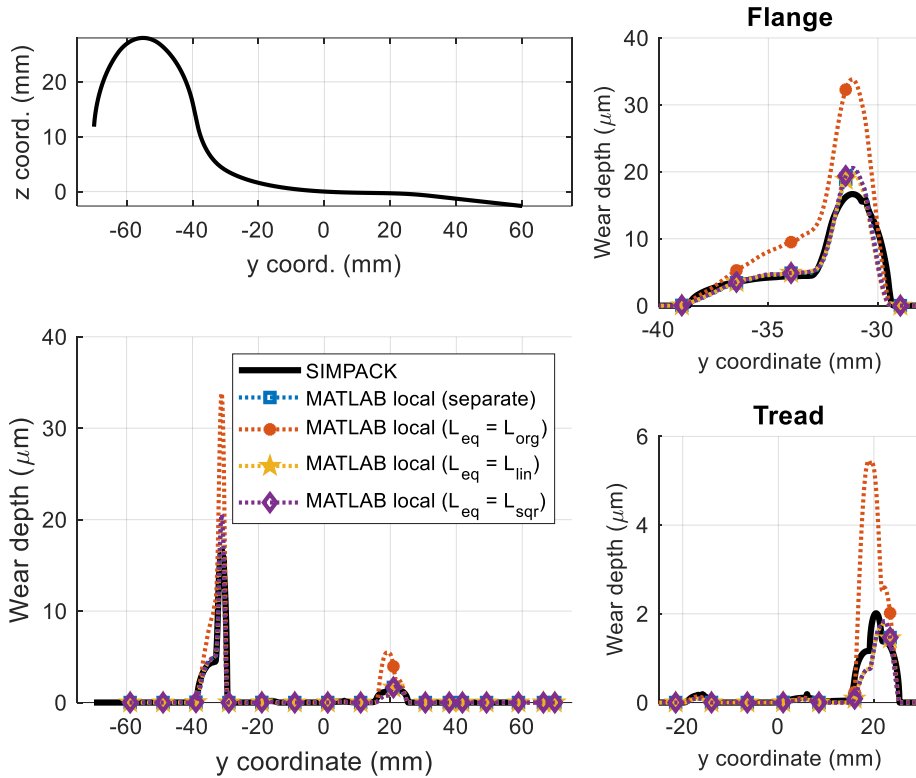


Figure 3: Effect of the different strategies to compute the slip speed magnitude.

Therefore, the calculations performed in the frame of this work suggest that the original expression provided by Kalker should be avoided, otherwise wear could be overestimated on both flange and wheel. This is in line with the outcomes of an activity carried out by Liu and Bruni [14], who proved that using three separate flexibilities is the best choice and leads to the best agreement with CONTACT in terms of sliding speed distribution on the contact patch. Nonetheless, the work by Liu and Bruni is predated with respect to the paper by Vollebregt and Voltr, so they could not test the new expressions. This work proves that the new expressions provide results that are in excellent agreement with the outputs obtained with separate flexibility in terms of wear.

Finally, in terms of computational times, the local wear algorithm is approximately 5 times slower with respect to the global approach, as the local method requires the discretization of the contact patch into adhesion and slip areas and the calculation of the tangential stresses and slip speed over the whole patch.

## 4 Conclusions and Contributions

The work shown in the present paper allows to benchmark the SIMPACK Wheel Profile Wear module and to tune in-house wear routines based on the local application of Archard's law, highlighting the differences with respect to global methods.

A first finding of this paper is that when using a single equivalent flexibility for the computation of the slip speed, the new expression introduced by Vollebregt and Voltr should be used, as the original equation can predict higher wear peaks, especially in mixed creepage conditions.

The local method predicts slightly larger wear peaks on the flange and lower wear on the tread, because it assigns a different wear zone to each element on the contact patch grid, while the global method can only identify a single wear regime for the whole patch.

The local wear method is not affected by peaks in the wear distribution produced when the number of contact patches changes during the simulation, because the local method identifies adhesion whereby the contact pressure is high.

Despite small deviations, the results obtained with the local and global methods are in good agreement with each other. The local method should be preferred when the simulation is intended to accurately predict the shape of the worn profile. However, it should be clarified whether the differences between the two methods are greater than the uncertainties in the calculation, such as those related to the wear coefficients, model parameters and algorithm for the solution of the wheel-rail contact problem.

The validated MATLAB routines for wear calculation can be adopted in future activities to gain control on the computation and to improve the stability of wear tools, still relying on the excellent reliability of commercial tools for the dynamic simulation.

## References

- [1] Pombo J, Ambrósio J, Pereira M, Lewis R, Dwyer-Joyce R, Ariaudo C, Kuka N (2010) A study on wear evaluation of railway wheels based on multibody dynamics and wear computation. *Multibody System Dynamics* 24 (3):347-366. <https://doi.org/10.1007/s11044-010-9217-8>
- [2] Pombo J, Ambrósio J, Pereira M, Lewis R, Dwyer-Joyce R, Ariaudo C, Kuka N (2010) A railway wheel wear prediction tool based on a multibody software. *Journal of Theoretical and Applied Mechanics* 48 (3):751-770
- [3] Pombo J, Ambrósio J, Pereira M, Lewis R, Dwyer-Joyce R, Ariaudo C, Kuka N (2011) Development of a wear prediction tool for steel railway wheels using three alternative wear functions. *Wear* 271 (1):238-245. <https://doi.org/10.1016/j.wear.2010.10.072>
- [4] Enblom R, Stichel S (2011) Industrial implementation of novel procedures for the prediction of railway wheel surface deterioration. *Wear* 271 (1):203-209. <https://doi.org/10.1016/j.wear.2010.10.037>
- [5] H-Nia S, Flodin J, Casanueva C, Asplund M, Stichel S (2024) Predictive maintenance in railway systems: MBS-based wheel and rail life prediction exemplified for the Swedish Iron-Ore line. *Vehicle System Dynamics* 61 (1):3-20. <https://doi.org/10.1080/00423114.2022.2161920>

- [6] Ye Y, Sun Y, Dongfang S, Shi D, Hecht M (2021) Optimizing wheel profiles and suspensions for railway vehicles operating on specific lines to reduce wheel wear: a case study. *Multibody System Dynamics* 51 (1):91-122. <https://doi.org/10.1007/s11044-020-09722-4>
- [7] Pires AC, Pacheco LA, Dalvi IL, Endlich CS, Queiroz JC, Antonioli FA, Santos GFM (2021) The effect of railway wheel wear on reprofiling and service life. *Wear* 477. <https://doi.org/10.1016/j.wear.2021.203799>
- [8] Bosso N, Magelli M, Zampieri N (2022) Simulation of wheel and rail profile wear: a review of numerical models. *Railway Engineering Science* 30 (4):403-436. <https://doi.org/10.1007/s40534-022-00279-w>
- [9] Bosso N, Zampieri N (2020) Numerical stability of co-simulation approaches to evaluate wheel profile evolution due to wear. *International Journal of Rail Transportation* 8 (2):159-179. <https://doi.org/10.1080/23248378.2019.1672588>
- [10] Kalker JJ (1982) A Fast Algorithm for the Simplified Theory of Rolling Contact. *Vehicle System Dynamics* 11 (1):1-13. <https://doi.org/10.1080/00423118208968684>
- [11] Jendel T (2002) Prediction of wheel profile wear—comparisons with field measurements. *Wear* 253 (1):89-99. [https://doi.org/10.1016/S0043-1648\(02\)00087-X](https://doi.org/10.1016/S0043-1648(02)00087-X)
- [12] Bosso N, Magelli M, Zampieri N (2022) Study on the influence of the modelling strategy in the calculation of the worn profile of railway wheels. In: Passerini G, Mera JM (eds). *WIT Transactions on The Built Environment*. WIT Press, Southampton (UK), pp 65-76. <https://doi.org/10.2495/CR220061>
- [13] Vollebregt E, Voltr P (2023) Improved accuracy for FASTSIM using one or three flexibility values. *Vehicle System Dynamics* 61 (1):309-317. [10.1080/00423114.2022.2042331](https://doi.org/10.1080/00423114.2022.2042331)
- [14] Liu B, Bruni S, Lewis R (2022) Numerical calculation of wear in rolling contact based on the Archard equation: Effect of contact parameters and consideration of uncertainties. *Wear* 490-491:204188. <https://doi.org/10.1016/j.wear.2021.204188>